

The Research on Air Curtain Structure Optimization Based on Computational Fluid Dynamics Simulation

Wu Shu^{*}, Wang Kun and Wang Chao

Suzhou Institute of Trade & Commerce, China

Keywords: Air curtain; Computational fluid dynamics (CFD); Structure optimization

Abstract: The uniformity of the distribution of airflow is mainly dependent on the shape and structure of the air curtain. Therefore, it is of great significance to study the structure of air curtain. But the study of the air curtain structure with great influence on the airflow has not been reported. The purpose of this paper is to study the wind speed distribution of air curtain under different air curtain structures by CFD numerical simulation. The results show that the best size for rounding at the entrance of the air curtain and the horizontal intersection is $r=520\text{mm}$, increase the baffle in the air curtain, and the best size is $R=250\text{mm}$. Finally, the optimized air curtain will be simulated again, and the reliability of the simulation results will be verified through experiments.

1. Introduction

Rice (*Oryza sativa*) is an important food crop worldwide [1]. In China, the total growing area of rice per year is approximately 29.4 million hectare, and the rice product amounts to approximately 200 billion kg [1]. Approximately 67% of the population in China depends on rice [2].

Agricultural intensification has aggravated the problems caused by biotic stressors, including insects and diseases, on rice [3]. In China, rice encounters many insect pests and suffers from various diseases, such as rice planthoppers, sheath blight, rice blast, rice borers and rice leaf folder. Rice planthoppers and rice sheath blight are the main insect pests and diseases of rice, respectively, and they occur in the middle and lower canopies of rice plant.

Air assistance has been considered a key element to improve the efficiency of spray application for dense crops [4]. Researchers have experimentally verified that the air delivery technique can effectively improve the crop canopy droplet distribution. Taylor and Andersen applied the air delivery technology to wheat and relied on airflow to improve the droplet velocity, increase canopy disturbance and achieve a better spray effect [5]. Ade et al. tested spray tomatoes by the air assistance technology, and the test results showed that the air assistance could significantly enhance the penetration of droplets and give a better distribution at different levels in dense foliage [6]. Van de zande et al. also applied the air delivery technique to potatoes, and the results shows that the air delivery technique could effectively increase the droplet deposition on the front and back of the middle and lower canopy leaves [7].

However, the distribution uniformity is the key parameters to determine the spray effect. The uniformity of the distribution of airflow is mainly dependent on the shape and structure of the air curtain. Therefore, it is of great significance to study the structure of air curtain. Computational fluid dynamics (CFD) has become an effective method for optimising the air delivery system and for solving the related research problems in recent years. It can be used for numerical simulation under controllable conditions. Delele M. A. et al. established a CFD model of the 3D airflow field of across-flow air sprayer and simulated the influence of the operating and fan speeds of the sprayer on the transient distribution of airflow velocity [8]. Donald D. et al. established a CFD model of the airflow droplet field of a wind-fed orchard sprayer and analysed the airflow velocity at different distances in front of the outlet [9]. The effect of canopy on airflow is necessary to consider to reflect the movement law of airflow and its interaction with canopy in CFD simulation. Endalew AM et al. established an integrated CFD model of an orchard sprayer [10]. The 3D model of the actual branch structure of peach canopy was introduced into the CFD model [11]. A porous subfield was created around the branches to indicate the small foliage of peach trees and simulate the effect of branch

portion on airflow [11]. The use of CFD to optimize the air sprayer is more, but the study of the air curtain structure with great influence on the airflow has not been reported.

The purpose of this paper is to study the velocity distribution of air curtain under different structures by CFD numerical simulation.

2. Air curtain structure CFD simulation

The length of the air curtain is 12 m, the shape and mechanism is shown in Fig. 1.

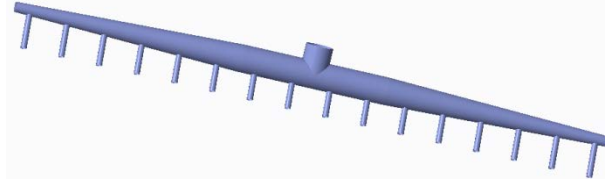


Figure 1 Air curtain shape and mechanism

The fluent CFD model [12] is used to calculate turbulent air flow characteristics. The fluent model has been applied to simulate air flow movement inside the air curtain. The simulation is based on Reynolds-averaged Navier-Stokes equations (RANS) and a standard steady state $k-\epsilon$ turbulence model [13].

In this paper, ANSYS software is used to extract the air curtain geometric model and establish the simulation model of air curtain. Because the structure of the air curtain is symmetrical, it is necessary to select the half of the air curtain structure for meshing and simulation, which effectively shortens the computational complexity of the simulation. The final simulation model shown in Fig.2. ICEM software is used to mesh the air curtain model. The mesh parameters are shown in Table 1.



Figure 2 Air curtain simulation model

Table 1 The mesh parameters

mesh type	mesh size	number of mesh	number of mesh nodes
hexahedron	1mm	1070927	167844
tetrahedron	1mm	267732	41962

The boundary condition refers to the law of the variable or the first derivative of the solution on the boundary of the solution domain with the location and time. Reasonable boundary conditions are the preconditions for the CFD stability to have a positive definite solution and the premise for the calculation of convergence and its possible implementation. The specific simulation setting types are shown in Table 2, and the simulation parameter settings are shown in Table 3.

Table 2 The simulation setting type

calculation model	inlet type	outlet type	material type
realizable $k-\epsilon$ turbulence model	velocity inlet	pressure outlet	air

Table 3 The simulation parameter setting

turbulent density	hydraulic diameter	reflux intensity	turbulent diameter	reflux diameter	hydraulic diameter	material density	dynamic viscosity
2%	120mm	2%	120mm	120mm	120mm	1.225kg/m ³	1.7894*10 ⁻⁵ Pa.S

3. Results and discussion

3.1. Air curtain simulation results

The airflow field velocity distribution and pressure distribution of air curtain are shown in Fig.3.

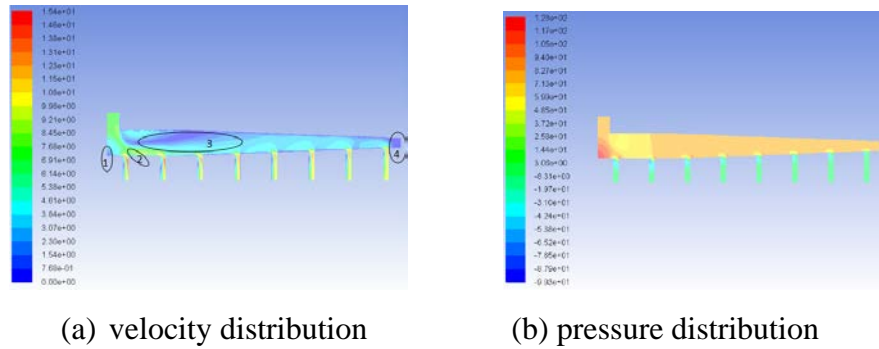


Figure 3 The airflow field velocity distribution and pressure distribution

As can be seen from Fig. 3, high-speed turbulence zones are created in zones 1 and 2 of the air curtain, and zones 3 and 4 produce a low velocity zone. This is because there is no arc transition between the vertical air inlet and the horizontal intersection of the air curtain. After the air flow enters, it is forced to move to Zone 1 and Zone 2 to form a high-speed turbulence zone. Since most of the airflow is moving to Zone 1 and Zone 2, it is bound to cause a low speed zone in Zone 3, which not only wastes energy, but also affects the uniformity of airflow in the wind screen.

Through the simulation analysis of the existing air curtain structure, the air curtain structure needs to be optimized as follows: 1, It is necessary to have an arc transition between the vertical air inlet and the horizontal intersection of the air curtain; 2, Increase the deflector in the middle of the curtain so as to force the velocity direction to move on both sides and reduce the high-speed area in Zone 2 and reduce the energy loss at the same time.

3.2. Optimization the size of arc

The radius of the air inlet of the air curtain is $r = 520\text{mm}$. The arcs were set up as follows: $r_1 = r = 520\text{mm}$, $r_2 = r/2 = 260\text{mm}$, $r_3 = r/3 = 173\text{mm}$, $r_4 = r/4 = 130\text{mm}$, $r_5 = r/5 = 104\text{mm}$. Based on different sizes, the corresponding air curtain simulation models are established respectively. According to the simulation parameter settings, the corresponding simulation is completed, and the result is shown in Fig. 4.

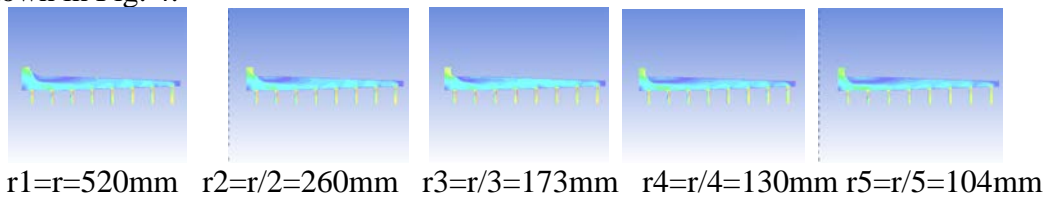


Figure 4 Airflow field distribution

According to the simulation results, three points are selected in Zone 1, Zone 2, and Zone 3, and the average velocity is counted. The specific results are shown in Table 4.

Table 4 Average velocity from three points

	Zone 1			Zone 2			Zone 3		
	1	2	3	1	2	3	1	2	3
r_1	18.1m/s	17.9m/s	17.5m/s	17.1ms/	16.9m/s	17.3m/s	16.8m/s	16.5m/s	16.3m/s
r_2	19.6m/s	19.8m/s	20.3m/s	18.5m/s	18.6m/s	20.1m/s	14.3m/s	14.6m/s	14.5m/s
r_3	20.2m/s	19.3m/s	19.8m/s	19.5m/s	19.2m/s	20.3m/s	12.5m/s	12.6m/s	12.1m/s
r_4	18.8m/s	19.5m/s	19.2m/s	20.5m/s	18.1m/s	19.8m/s	10.6m/s	11.1m/s	10.9m/s
r_5	19.1m/s	18.6m/s	20.2m/s	20.8m/s	19.6m/s	18.1m/s	10.9m/s	9.8m/s	8.6m/s

According to the analysis of different simulation results, when $r = 520\text{mm}$, the high-speed

turbulence zone in zone 1 and zone 2 basically disappears and the low-velocity zone in zones 3 also decreases. So determine $r=520\text{mm}$ as the best size for the arc.

3.3. Increase the baffle into air curtain and optimization the size of the baffle

Increasing the baffle in the air curtain structure will force the velocity direction to move on both sides, thus reducing the high-speed turbulence area in the 2 areas and reducing the energy loss. As shown in Fig. 5, the structure of the baffle is located symmetrically in the middle of the air curtain, and the structure of the air curtain after the baffle is added is shown in Fig. 6. However, the size of the baffle has an important influence on the flow field. Therefore, the distribution of the airflow field under different baffle radians is analysed through simulation.



Figure 5 Baffle structure

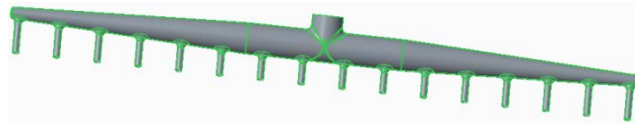


Figure 6 Air curtain with Baffle structure

In order to obtain the best baffle radius size, it is necessary to study the influence of the baffle on the distribution of the airflow field. The diameter of the middle part of the air curtain is $r = 520\text{mm}$. Therefore, the baffle size is set to $R1 = 400\text{mm}$ and $R2 = 350\text{mm}$, $R3 = 300\text{mm}$, $R4 = 250\text{mm}$, $R5 = 200\text{mm}$ respectively. Based on different sizes, the corresponding air curtain simulation models are established respectively. According to the simulation parameter settings, the corresponding simulation is completed, and the result is shown in Fig. 7.

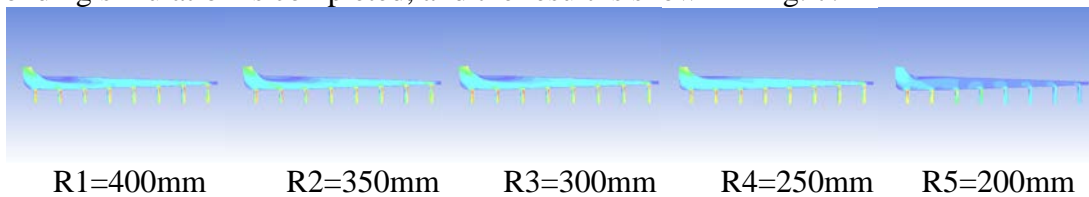


Figure 7 Airflow field distribution with baffle

According to different simulation analysis, when $R4 = 250\text{mm}$, the result of air curtain simulation is the best. The low velocity region in Zone 3 decreases, and the flow field distribution is the most uniform throughout the air curtain. Therefore, the baffle size is finally set to $R=250\text{mm}$.

3.4. Simulation the optimized air curtain ($r=520\text{mm}$, $R=250\text{mm}$)

Based on the previous simulation analysis, the optimal size of the arc of the air curtain inlet and the horizontal intersection is determined, the baffle size is determined. Based on sizes, the corresponding air curtain simulation model is established respectively. According to the simulation parameter settings, the corresponding simulation is completed, and the result is shown in Fig. 8.

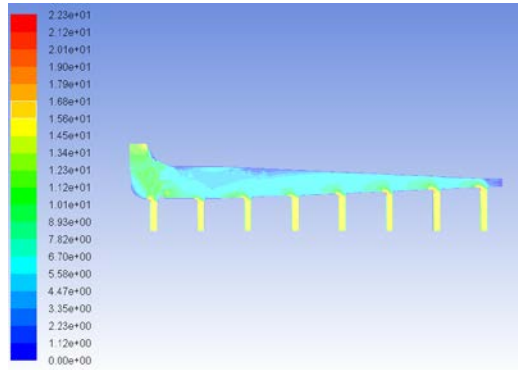


Figure 8 Airflow field distribution ($r=520\text{mm}$, $R=250\text{mm}$)

According to the simulation analysis, the air velocity of each air outlet is uniform, and the air velocity of each air outlet is 14-15m/s. And the flow field in the whole air curtain is distributed evenly, and the range of low-speed area and high-speed area are effectively reduced.

In order to verify the reliability of the simulation results, this paper verifies the simulation results of this paper through experiments.

4. Experimental verification

4.1. Compare the results before optimization with the after optimization

In order to verify the reliability of the simulation analysis, the air flow velocity at different positions of the air curtain outlet was tested. Set different monitoring points at each air curtain outlet. Monitoring points are respectively set in the horizontal directions of 0mm, 10mm, 50mm and 100mm from the air curtain outlet height respectively. The specific monitoring points are distributed as shown in Fig. 9. The test results show the velocity profiles at different horizontal sections before optimization and after optimization, as shown in Fig. 9.

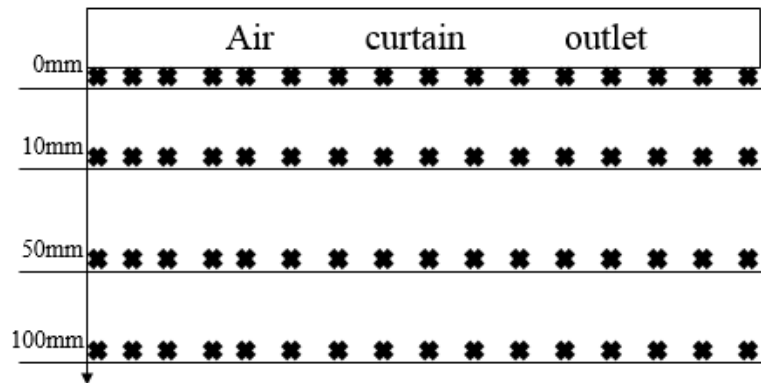
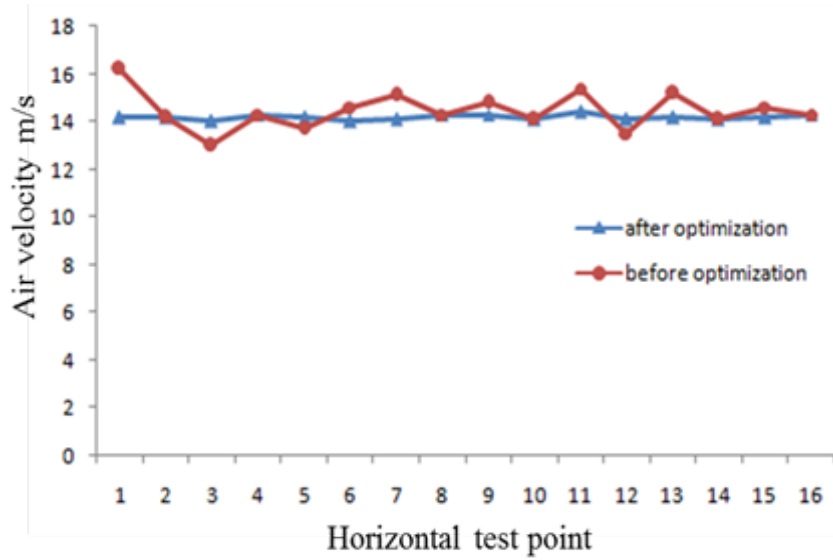
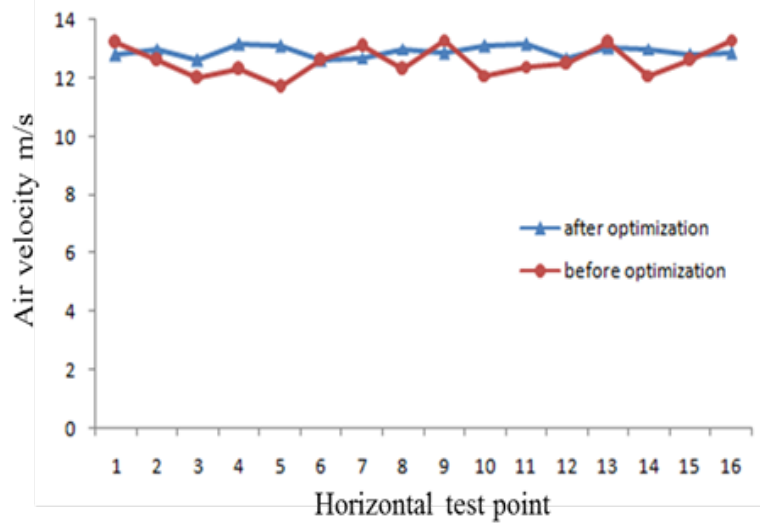


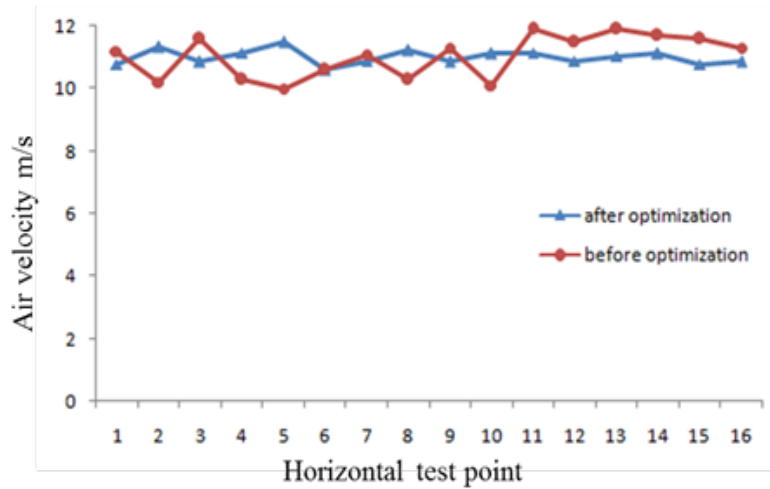
Figure 9 Monitoring point distribution



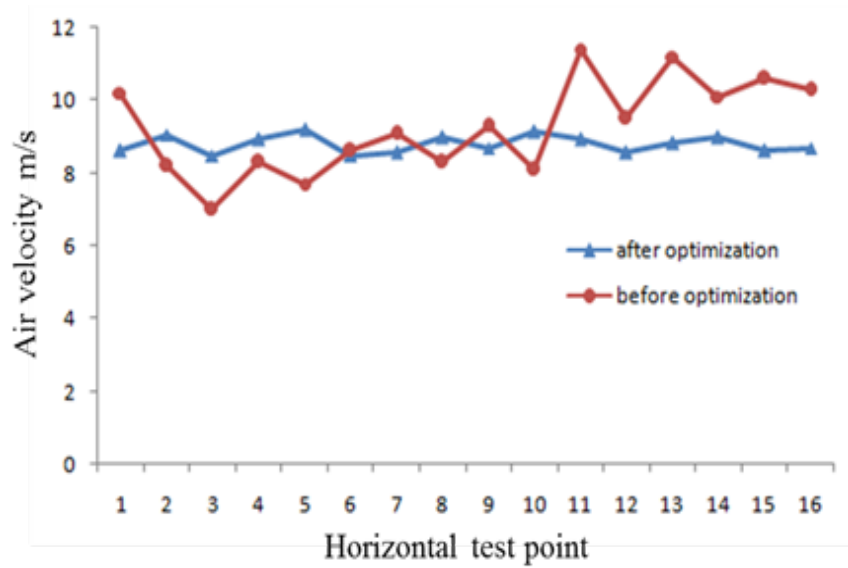
(a) The distance of 0mm



(b) The distance of 10mm



(c) The distance of 50mm



(d) The distance of 100mm

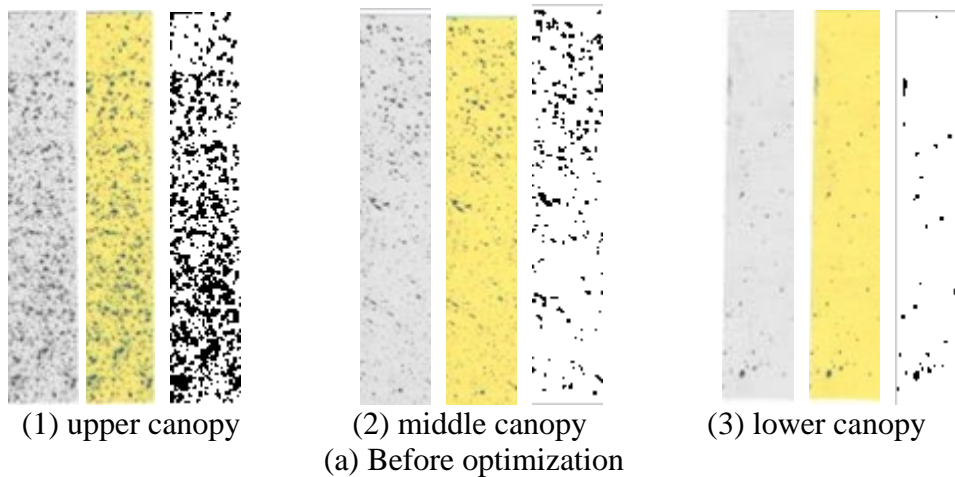
Figure 10 The test results show the velocity profiles at different horizontal sections

It can be seen from Fig. 10 that at the different height from the outlet of the air curtain, the distribution of the outlet airflow field in the optimized air curtain structure is more uniform. Effectively improve the uneven distribution of the airflow field before optimization.

At a distance of 0mm from the air curtain outlet, the air velocity distribution is basically linear distribution. At the distance of 10mm, 50mm and 100mm from the outlet of the air curtain, the air velocity distribution is basically the same, with irregular fluctuations. When the farther away from the outlet of the air curtain, the greater the fluctuation amplitude, the lower the average velocity of the air stream. The main reason is that the test results are affected by the natural environment and other factors. On the whole, the airflow distribution is better after optimization.

4.2. Compare the field experiment results before optimization with after optimization

In order to test the deposition distribution, water-sensitive paper were used to test the deposition in field. Arrange the corresponding test points on each canopy. Fig. 11 were the droplet deposition before optimization and after optimization. The experiment shows that the droplet deposition rate distribution of the upper canopy before optimization is relatively uniform, the droplet deposition in the middle and lower canopy is less, and the distribution is not uniform. After optimization, the deposition amount of the droplet on the upper part, the middle part and the lower part of the crop canopy increased and was more uniform.



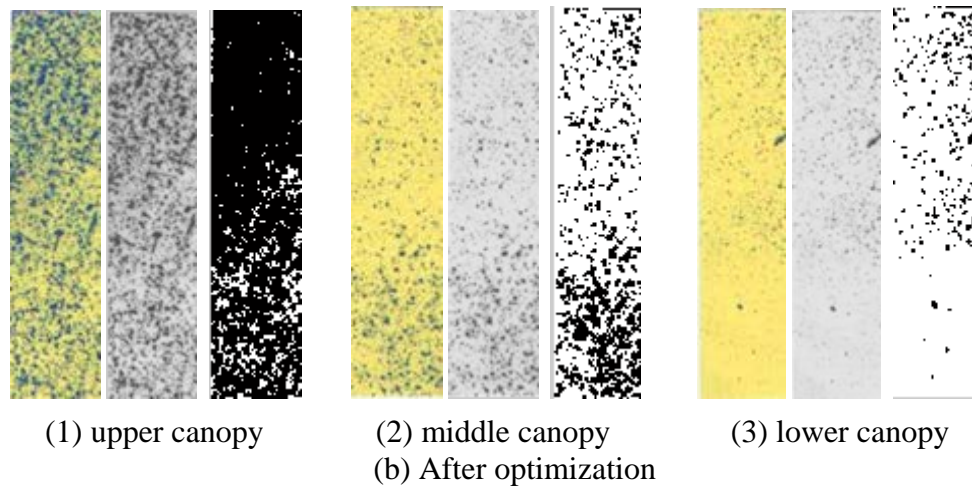


Figure 11 The deposition distribution before and after optimization

Through the treatment of the field test data and the calculation of the average droplet deposition volume of each canopy, the average values of the droplet deposition amount of each canopy before and after optimization are respectively given in Table 5.

Table 5 The droplet deposition rate of each canopy

Location	upper canopy		middle canopy		lower canopy	
	before	after	before	after	before	after
Rate of deposition	69.01%	79.29%	44.51%	70.92%	39.83%	69.04%

5. Conclusion

In this paper, the air curtain as the research object, the use of CFD numerical simulation to study the air curtain optimization. Finally obtained the following conclusion:

1) The best size for rounding at the entrance of the air curtain and the horizontal intersection is $r=520\text{mm}$;

2) Increase the baffle in the air curtain, and the best size is $R=250\text{mm}$.

3) When the baffle is added in the middle of the air curtain, and the $r=520\text{mm}$, $R=250\text{mm}$, the simulation result of the air curtain structure is the best, and the distribution of the flow field inside the air curtain is the most uniform.

References

- [1] Yong-Gen Lou, Gu-Ren Zhang, Wen-Qing Zhang, Yang Hu, Jin Zhang. Reprint of: Biological control of rice insect pests in China. *Biological Control*, 2014, 68: 103-116.
- [2] Hu, L.Y., Ding, Y.F. *Crop Cultivation*. Beijing: High Education Press, 2008: 490.
- [3] K. Selvaraj, Subhash Chander, M. Sujithra. Determination of multiple-species economic injury levels for rice insect pests. *Crop Protection*, 2012, 32: 150-160.
- [4] Jordi Llop, Emilio Gil, Montserrat Gallart, Felipe Contador, Mireia Ercilla. Spray distribution evaluation of different setting of a hand-held trolley sprayer used in greenhouse tomato crops. *Pest Management Science*, 2015, 72: 505-516.
- [5] Taylor W A, Andersen P G. A review of benefits of air assisted spraying trials in arable crops. *Aspects of Applied Biology*, 1997, 48: 163-174.
- [6] Ade G, Pezzi F, Taylor W A, Cooper S E. The influence of some application variables on spray deposition in field-grown tomatoes. *Aspects of Applied Biology*, 2000, 57: 225-233.
- [7] Van de Zande J C, Michielsen J M G P, Stallinga H, Porskamp H A J, Holterman H J, Huijsmans J F M. Spray distribution when spraying potatoes with a conventional or an air-assisted

boom sprayer. ASAE Paper no 021003, 2002 Annual Meeting, 2002.

[8] Delele MA., Moor A De, Sonck B., et al. Modelling and validation of the air flow generated by a cross flow air sprayer as affected by travel speed and fan speed. *Biosystems Engineering*, 2005, 92(2): 165-174.

[9] Donald D., Ashenafi T.D., Pieter V., et al. Assessment of orchard sprayers using laboratory. *Biosystems Engineering*, 2013, 114: 157-169.

[10] Endalew A M., Debaer C., Rutten N. A new integrated CFD modelling approach towards air-assisted orchard spraying. Part I. Model development and effect of wind speed and direction on sprayer airflow. *Computers and Electronics in Agriculture*, 2010, 71: 128-136.

[11] Endalew A M., Debaer C., Rutten N. A new integrated CFD modelling approach towards air-assisted orchard spraying. Part II. Validation for different sprayer types. *Computers and Electronics in Agriculture*, 2010, 71: 137-147.

[12] Fluent Inc. FLUENT 6.2 user's guide, volumes 1–3, Fluent Inc., Lebanon, 2005, 2216.

[13] Jose Luis Santiago, Alberto Martilli, Fernando Martin. CFD simulation of airflow over a regular array of cubes. Part I: Three-dimensional simulation of the flow and validation with wind-tunnel measurements. *Boundary-Layer Meteorol*, 2007, 122: 609-634.